# Anisotropic flow measurements in Pb+Pb @ 13*A* and 30*A* GeV/*c* with NA61/SHINE

Oleg Golosov

(*NRC "Kurchatov Institute", MEPhI*)

for the NA61/SHINE Collaboration

NATIONAL RESEARCH CENTER "KURCHATOV INSTITUTE"

MEPhI

NICA-2024

# Outline

- Anisotropic flow observable
- World data
- NA61/SHINE experiment
- Analysis description
  - Datasets, event and track selection
  - Centrality and particle identification
  - Flow measurement procedure and acceptance corrections
- Results
- Model comparison

# Collision geometry and the anisotropic transverse flow

Asymmetry in coordinate space converts due to interaction into momentum asymmetry with respect to the reaction plane (help constrain transport properties of QCD matter):

$$\rho(\phi) = \frac{1}{2\pi}\left(1 + 2\sum_{n=1}^{\infty} v_n \cos\left[n(\varphi - \Psi_{RP})\right]\right) \qquad v_n = \langle \cos n(\varphi - \Psi_{RP}) \rangle$$

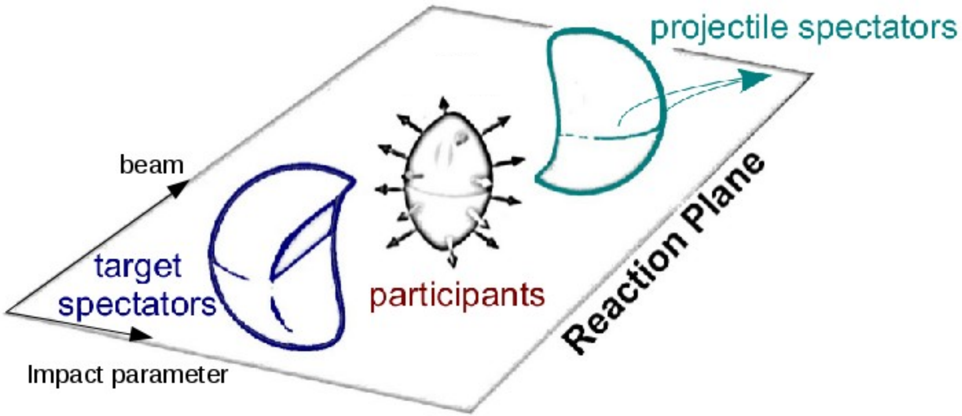


Components needed to calculate $v_n$

- momentum ($\phi$, $y$, $p_T$)
- centrality estimation
- particle identification
- $\Psi_{RP}$ estimate with symmetry planes of
  - participants
  - projectile / target spectators

# Collective flow at different energies

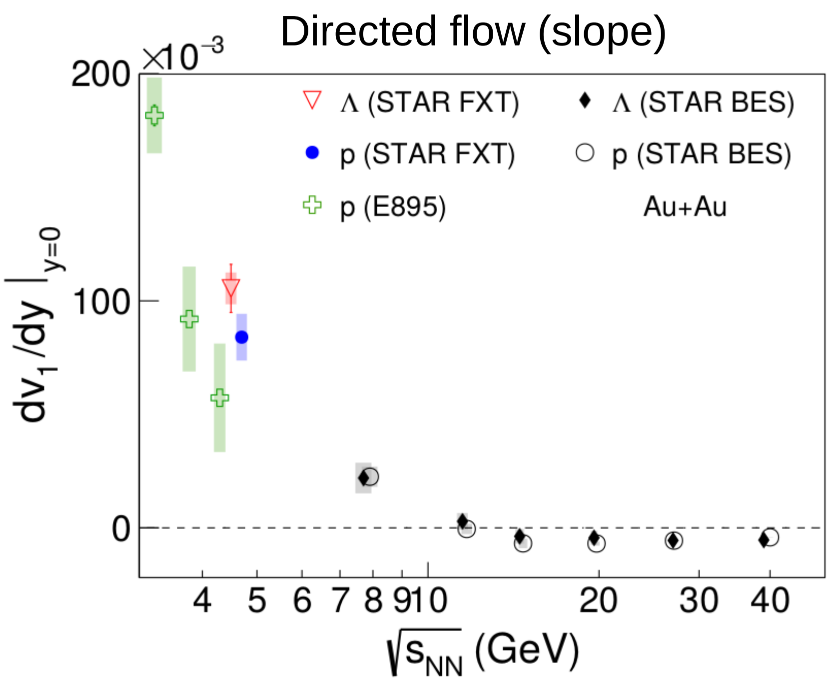


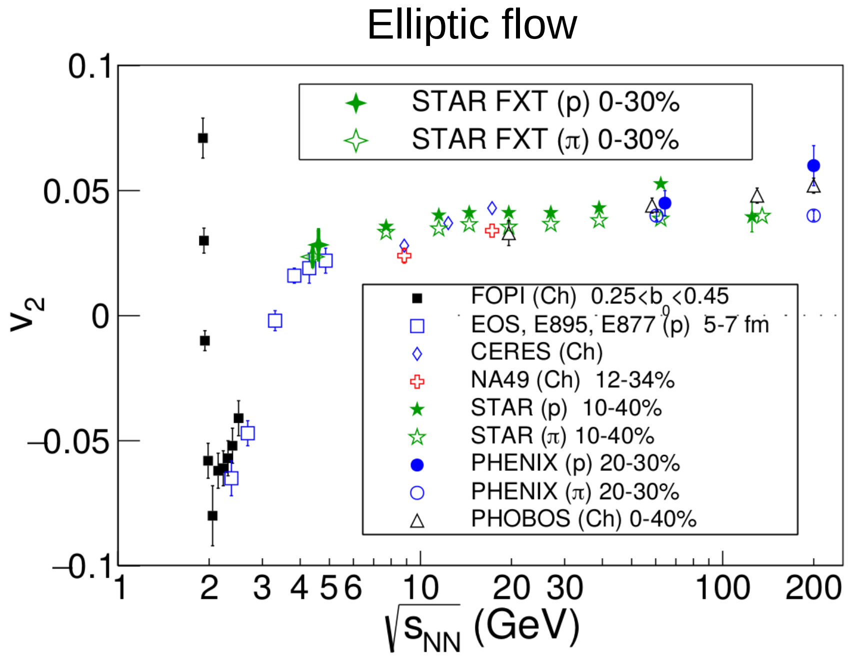


STAR Collaboration, PRC 103, 034908 (2021)

- NA61/SHINE Pb-ion beam energy scan: $p_{LAB}$ = 13-150*A* GeV/*c* ($\sqrt{s_{NN}}$ = 5.1-16.8 GeV)
  - complementary to STAR@RHIC and future NICA beam energies
- Advantage of fixed target setup
  - forward rapidity tracking with TPC
  - projectile spectators energy with forward calorimeter

# Collective flow at different energies

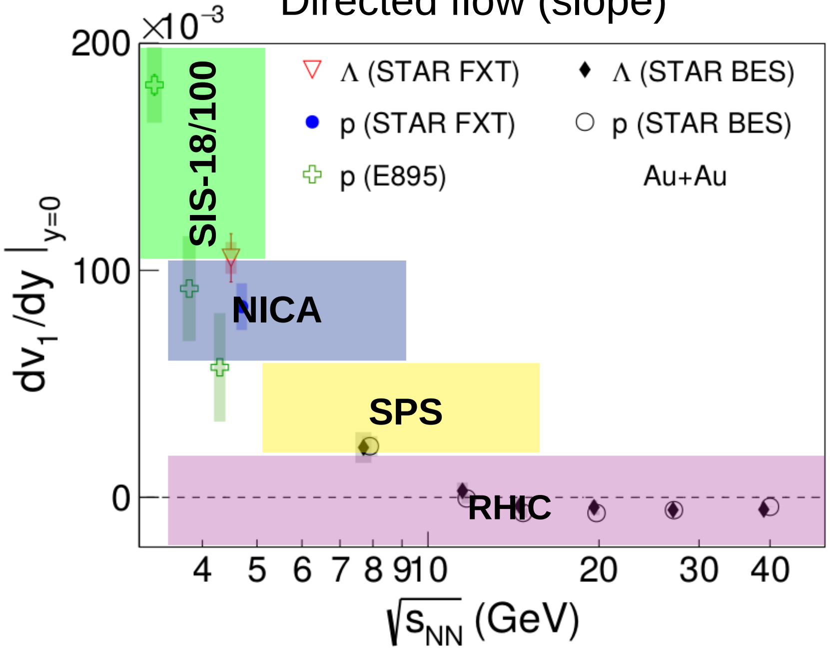


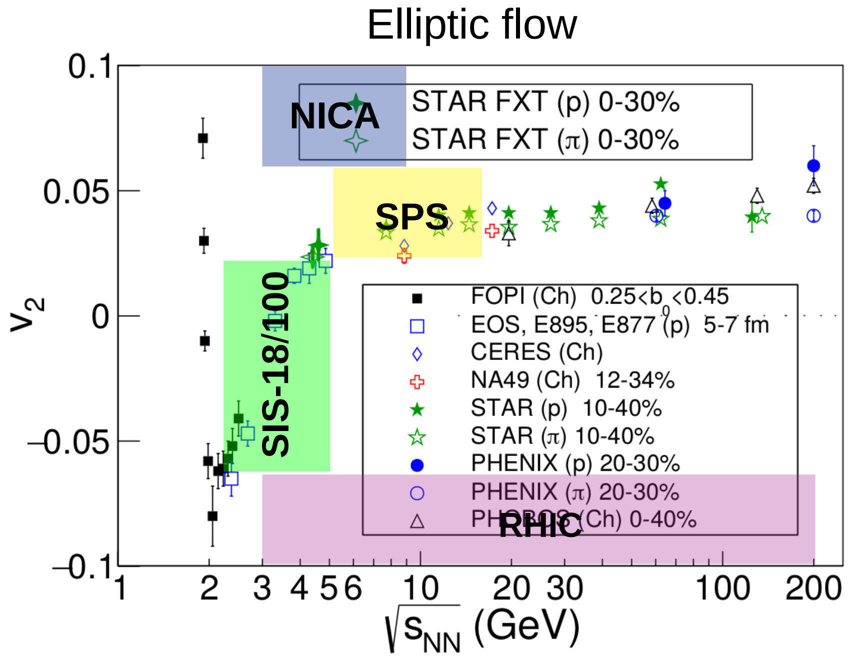


STAR Collaboration, PRC 103, 034908 (2021)

- NA61/SHINE Pb-ion beam energy scan: $p_{LAB}$ = 13-150*A* GeV/*c* ($\sqrt{s_{NN}}$ = 5.1-16.8 GeV)
  - complementary to STAR@RHIC and future NICA beam energies
- Advantage of fixed target setup
  - forward rapidity tracking with TPC
  - projectile spectators energy with forward calorimeter

# NA61/SHINE experiment at CERN SPS

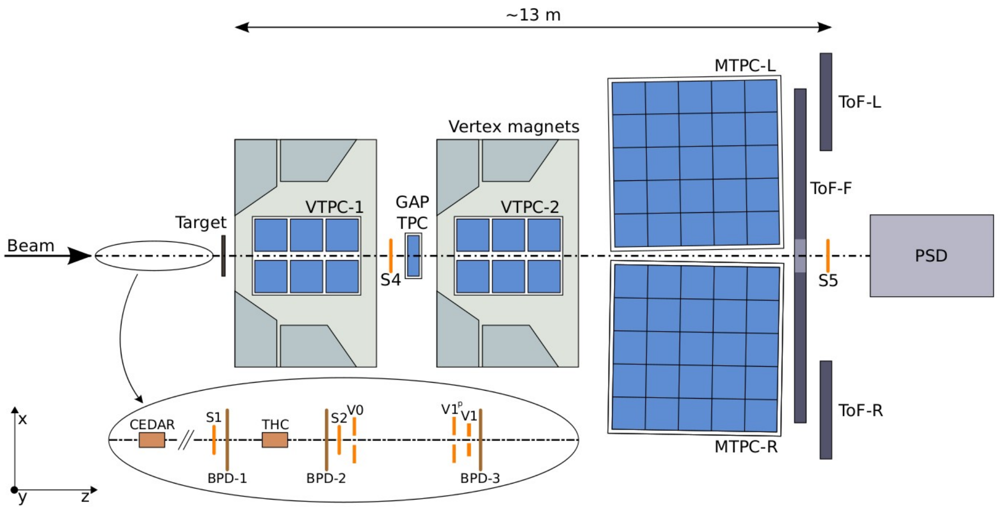


Projectile Spectator Detector (PSD)

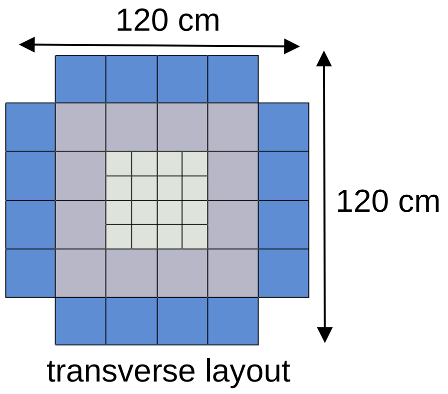


- Large acceptance hadron spectrometer (TPC)
  - full coverage of forward hemisphere
  - tracking + identification with dE/dx down to $p_T$ ~ 0 GeV/*c*
- Forward rapidity calorimeter with transverse granularity (PSD)
- Pb+Pb beam momentum scan: 13*A*, 30*A*, 150*A* GeV/*c* ($\sqrt{s_{NN}}$ = 5.1, 7.6, 16.8 GeV)
- System size scan (Xe+La, Ar+Sc, Be+Be)

# Analysis description

# Datasets, event and track selection

**Datasets:** Pb+Pb @ 13*A* and 30A GeV/c ( $\sqrt{s_{NN}}$ = 5.1 and 7.6)

**Event selection:**

- Central or minbias trigger
- Rejection of pileup and upstream ineraction: no hits in beam counters in 4 ms around trigger, graphical cuts on signal in beam counters and on $E_{PSD}$ vs Ntracks
- Perfect fit of PV, $Z_{vtx}$ < 2 cm from nominal, $X_{vtx}$ and $Y_{vtx}$ within 3 sigma from run mean

**Track selection:**

- Nclust > 30, NclustVTPC > 15, 0.55 < Nclust / NclustPotential < 1.1
- $\chi^2 < 10^5$
- $|DCA_X| < 2$ cm, $|DCA_Y| < 1$ cm

# Centrality estimation

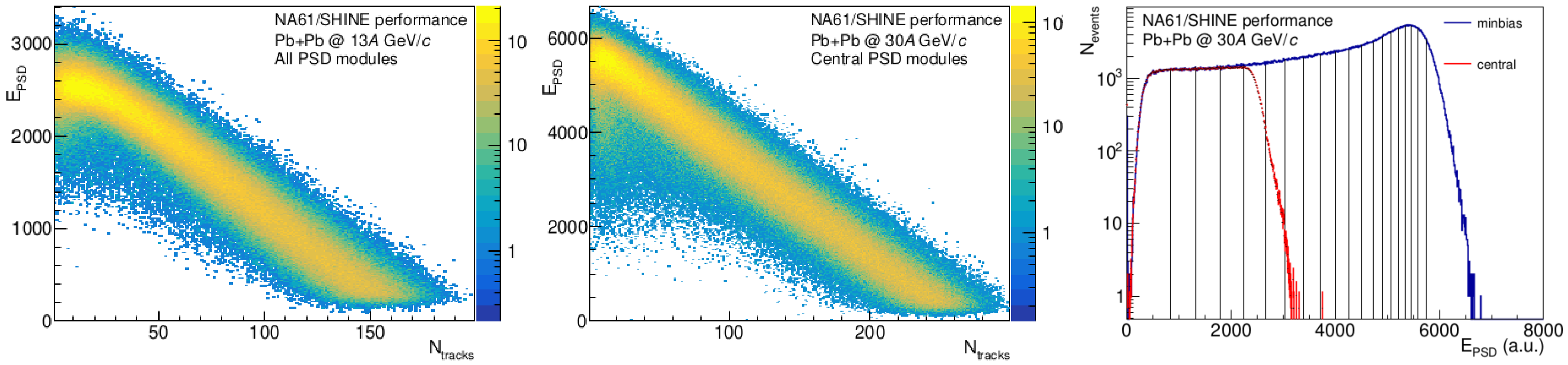


- Based on energy deposition in all (13A GeV/c) and central (30A GeV/c) PSD modules
- Clear anti-correlation with number of tracks – main contribution from spectators
- PSD saturation in the most peripheral events due to large spectator fragments

# Particle identification with identity method

Negative charge

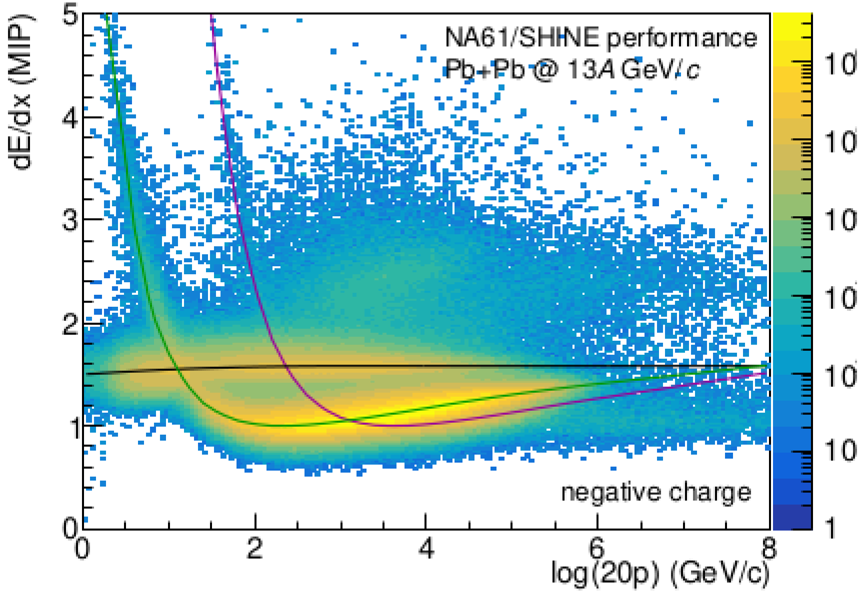


Positive charge

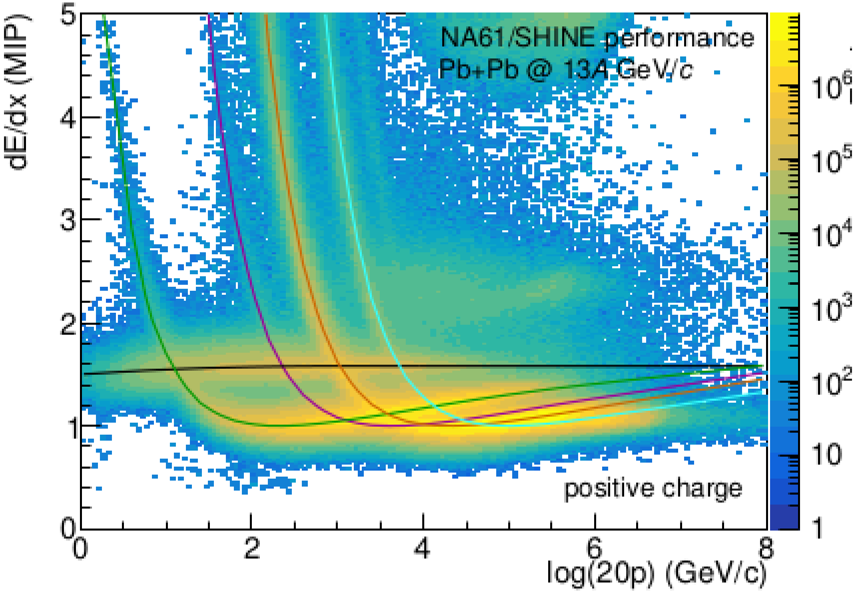


Fitting is performed in bins of log(20p)

# Particle identification with identity method

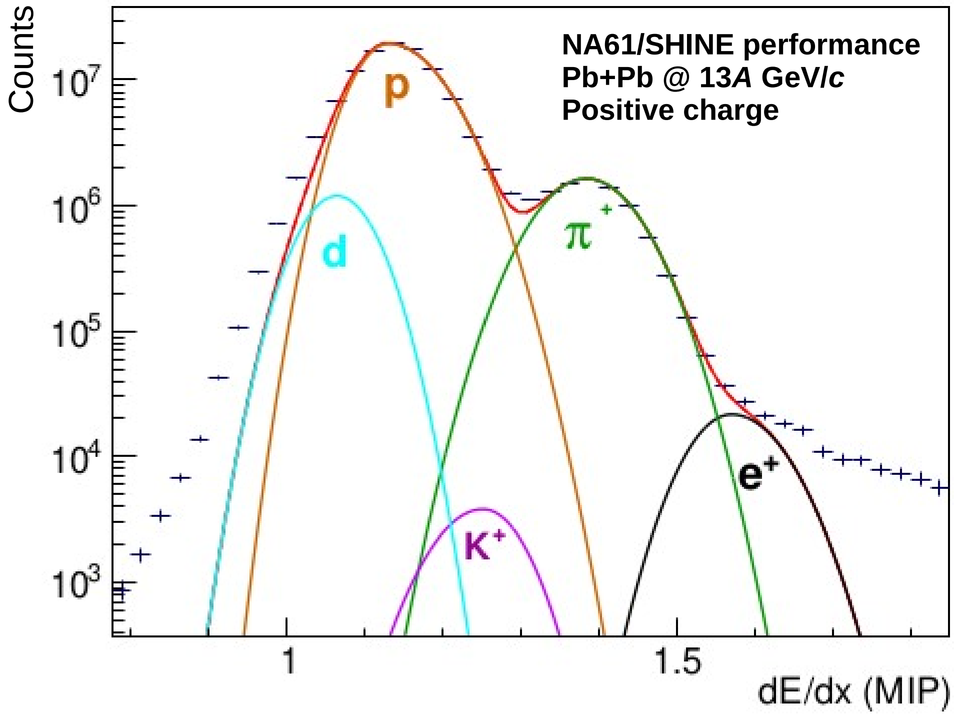


Fit example for positively charged tracks in 5.8 < log(20p) < 5.85 GeV/*c*

# Particle identification with identity method

Negative charge

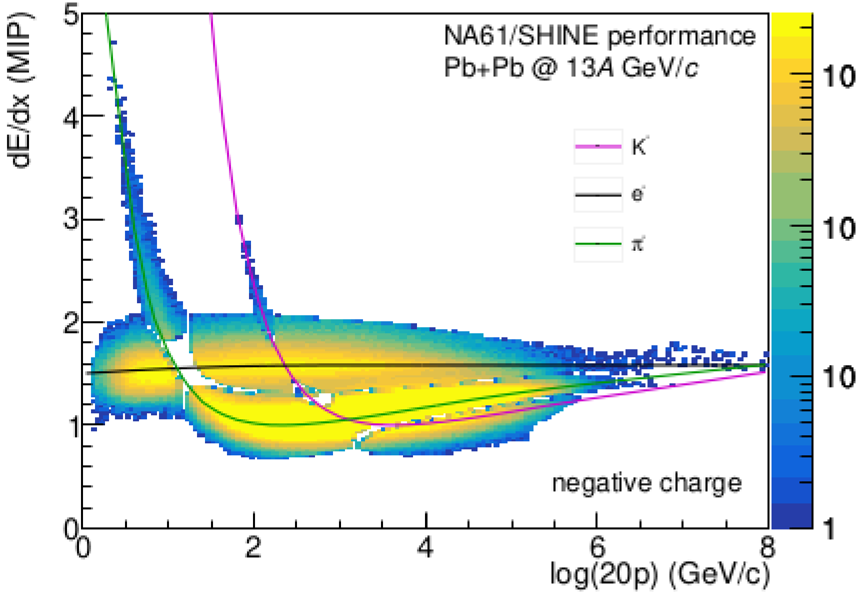


Positive charge

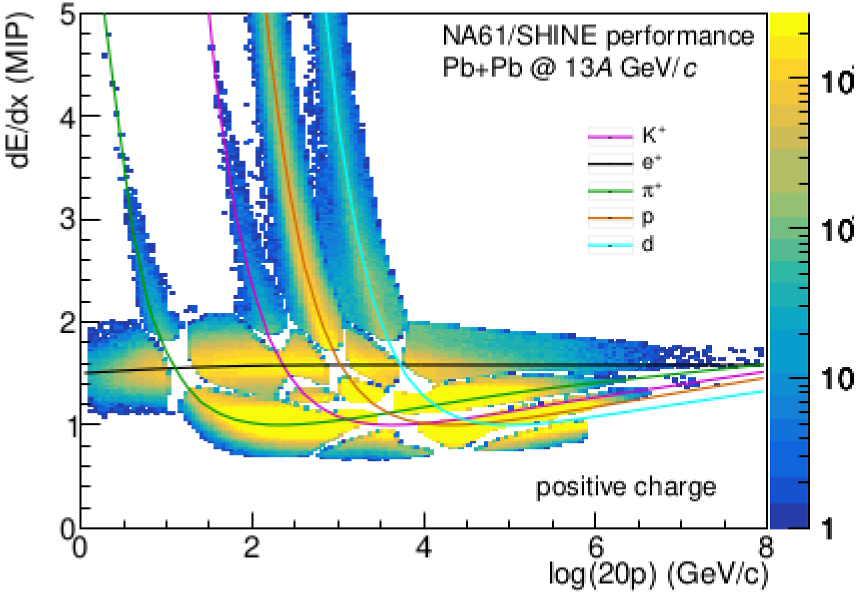


Particle selections with 90% purity

# Scalar product method with 1st harmonic Q-vector

**$u$-vector**

$$\mathbf{u_n} = (u_{n,x}, u_{n,y}) = (\cos(n\phi), \sin(n\phi))$$

$\varphi$ - azimuthal angle of particle momentum (or PSD module)

**PSD subevents $Q_1$-vector**

$$Q^S_{1,\alpha} = \frac{1}{\sum E_i} E_i u^{\alpha}_{1,i}$$

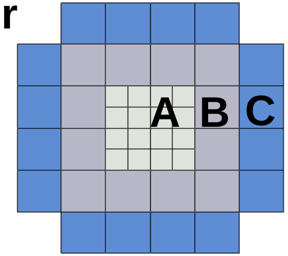


$S$ = A,B,C – PSD subevents

$i$ - index of PSD module in subevent

$$\alpha, \beta, \gamma = x, y$$

**Directed flow:**

$$v_{1,\alpha}\{S\} = \frac{2\langle u_{1,\alpha} Q^S_{1,\alpha} \rangle}{R^S_{1,\alpha}}$$

6 independent combinations

**Elliptic flow:**

$$v_{2,\alpha\beta\gamma}\{S1, S2\} = \frac{4\langle u_{2,\alpha} Q^{S1}_{1,\beta} Q^{S2}_{1,\gamma} \rangle}{R^{S1}_{1,\beta} R^{S2}_{1,\gamma}}$$

12 non-zero combinations

$R_1^S$ – resolution correction factor for the subevent $S$ *(see the following slides)*

# Data driven corrections for detector azimuthal non-uniformity

protons

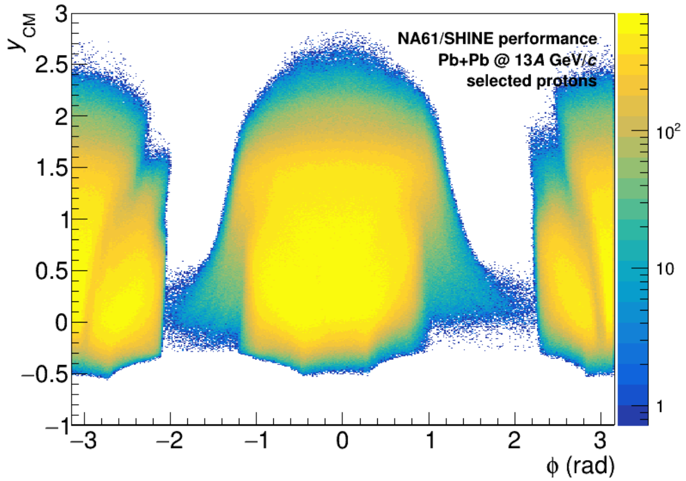


negative pions

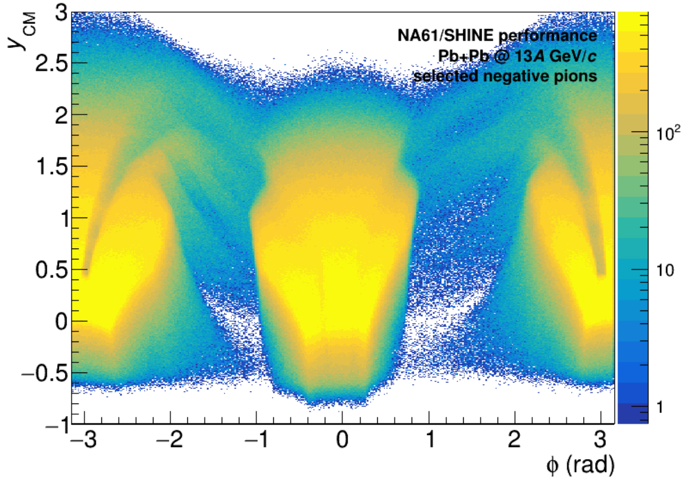


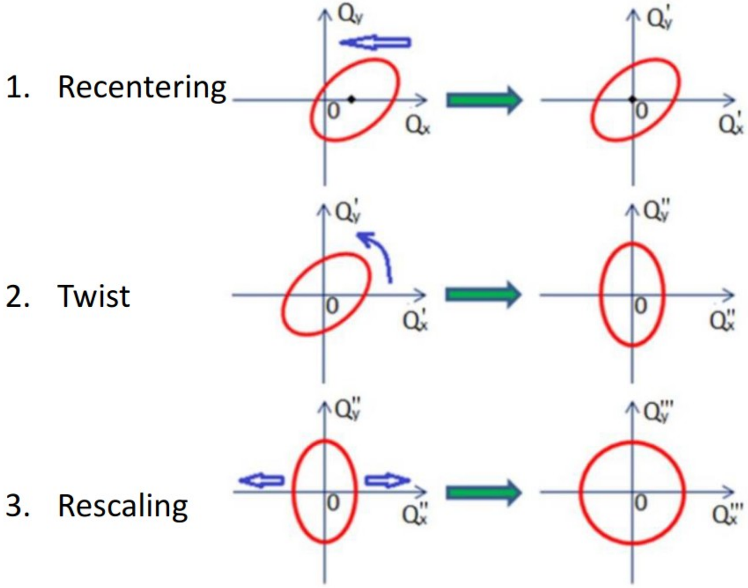


I. Selyuzhenkov and S. Voloshin [PRC77 034904 (2008)]

Recentering, twist, and rescaling corrections applied
time dependent (run-by-run) and as a function of $p_T$, $y$ and centrality

# 3 PSD subevents resolution

NA61 PSD

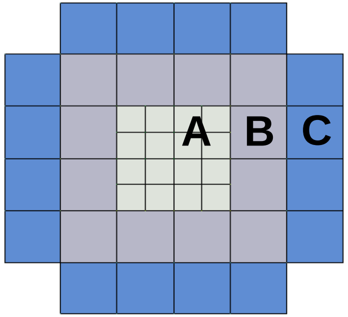


$$R_{1,\alpha}^{A} = \sqrt{\frac{\langle Q_{1,\alpha}^{A} Q_{1,\alpha}^{C} \rangle \langle Q_{1,\alpha}^{A} Q_{1,\alpha}^{B} \rangle}{\langle Q_{1,\alpha}^{B} Q_{1,\alpha}^{C} \rangle}}$$

$$\alpha = x, y$$

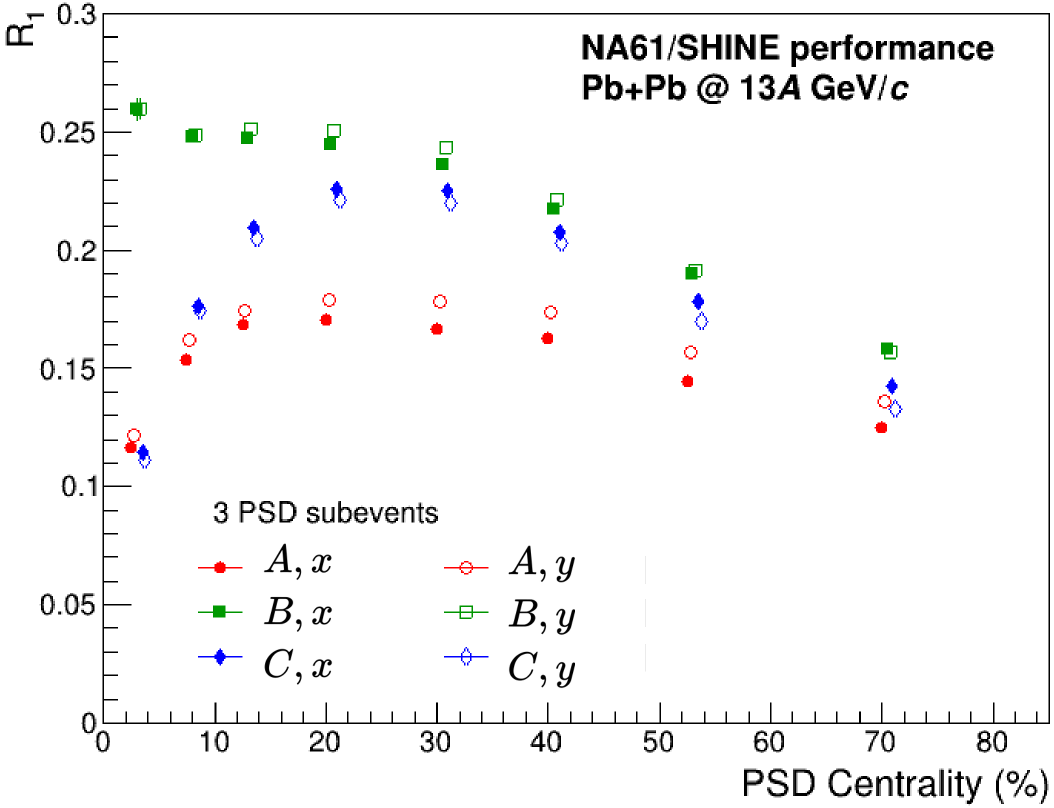


- Resolution correction is biased due to spread of hadronic shower across PSD subevents.
- Pseudorapidity separation of subevents is required.

# 3 PSD + 1 TPC subevents resolution

PSD

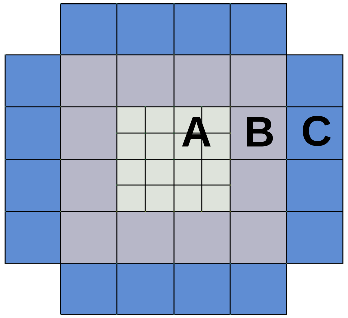


+ $Q_1^{TPC}$

protons

$0.8 < y < 1.2$

$p_T > 0$

$$R_{1,\alpha}^{A,C} = \sqrt{\frac{\langle Q_{1,\alpha}^{A} Q_{1,\alpha}^{C}\rangle \langle Q_{1,\alpha}^{A,C} Q_{1,\alpha}^{T}\rangle}{\langle Q_{1,\alpha}^{T} Q_{1,\alpha}^{C,A}\rangle}} \quad R_{1,\alpha}^{B} = \frac{\langle Q_{1,\alpha}^{B} Q_{1,\alpha}^{T}\rangle}{R_{1,\alpha}^{T}}$$

TPC subevent resolution:

$$R_{1,\alpha}^{T} = \sqrt{\frac{\langle Q_{1,\alpha}^{T} Q_{1,\alpha}^{C}\rangle \langle Q_{1,\alpha}^{T} Q_{1,\alpha}^{B}\rangle}{\langle Q_{1,\alpha}^{B} Q_{1,\alpha}^{C}\rangle}} \qquad \alpha = x, y$$

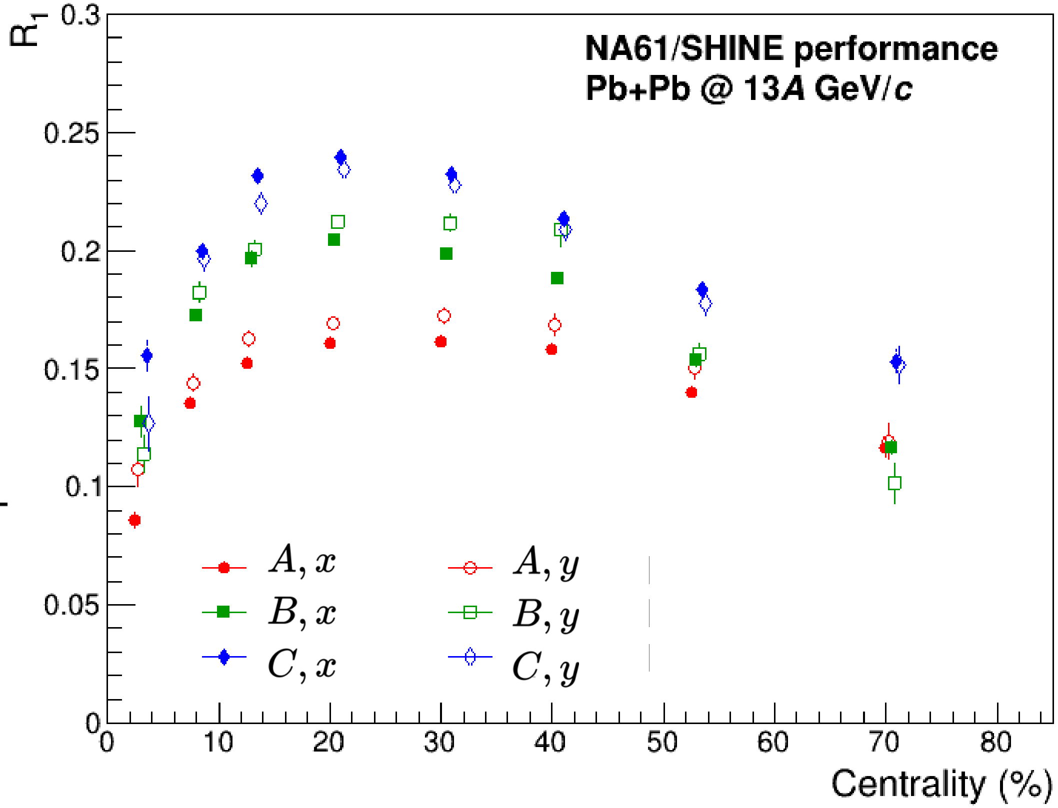


Additional correlations are suppressed by using pseudorapidity-separated subevents.

# Tracking efficiency

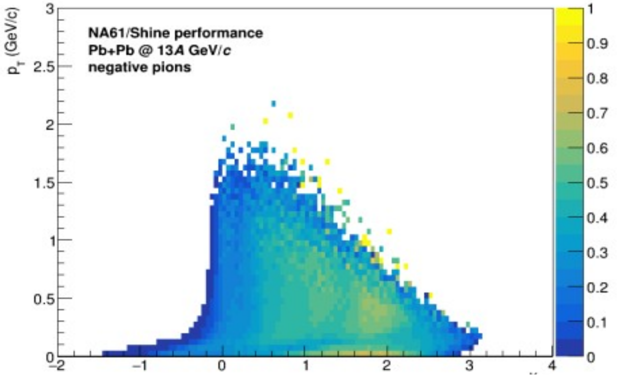


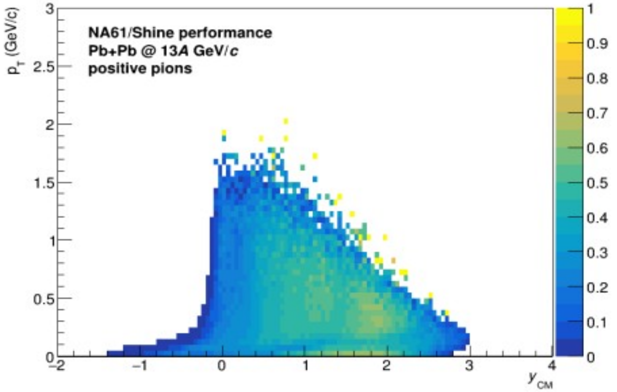


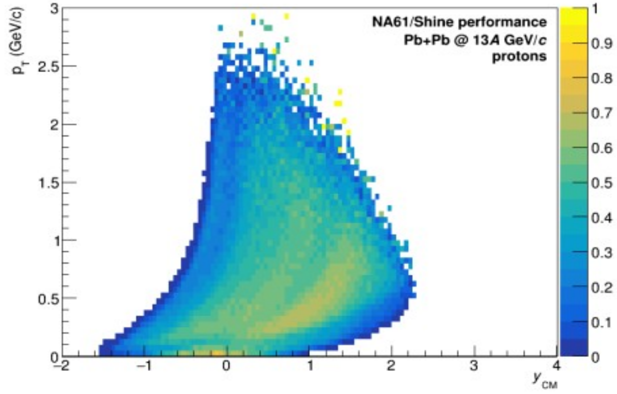


$$\varepsilon_i(p_T, y_{CM}) = \frac{N^i_{reco}(p_T, y_{CM})}{N^i_{sim}(p_T, y_{CM})}$$

$$w_i(y_{CM}, p_T) = 1/\varepsilon_i(p_T, y_{CM})$$

$$\mathbf{Q}_n = \frac{1}{M}\sum_i^N w_i \mathbf{u}_{n,i}, \quad M = \sum_i^N w_i$$

Trecking efficiency correction is applied as a weight in **Q**-vectors (slide 12)

# Sources of systematics: **Q**-vector component variation

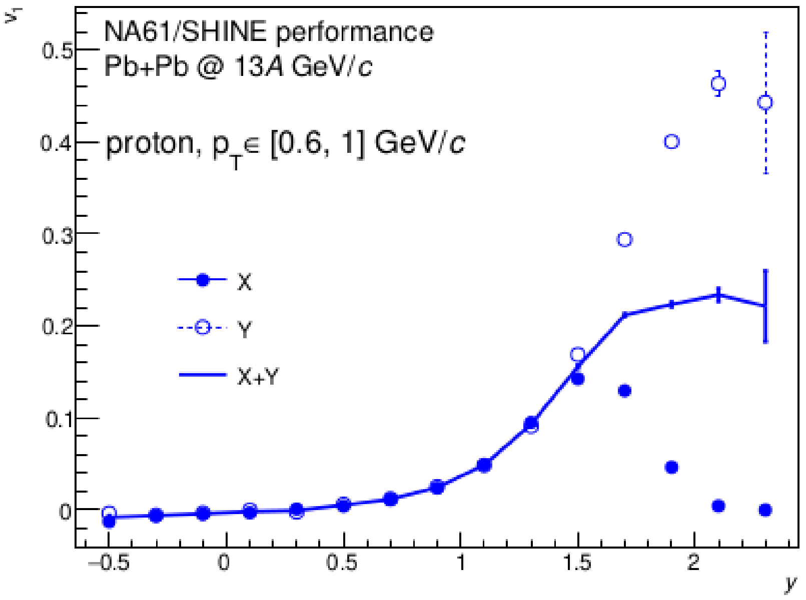


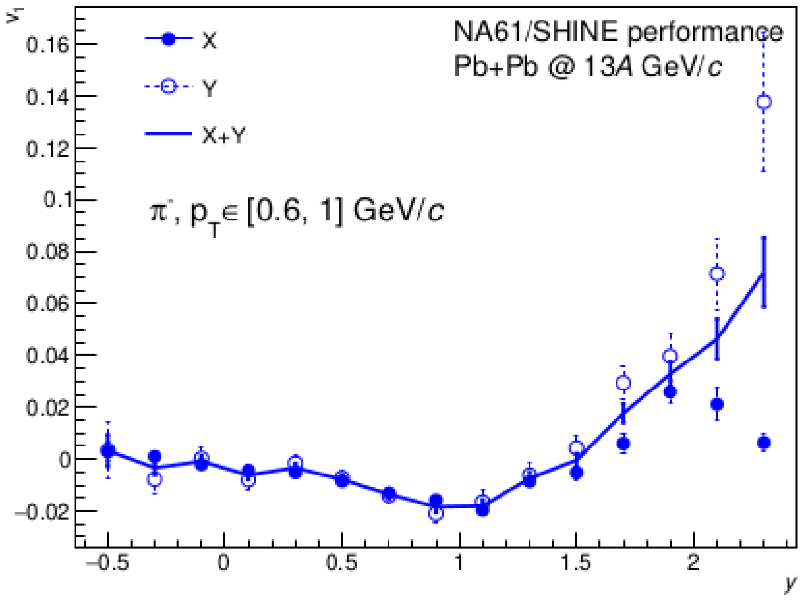


Difference originates from the acceptance anisotropy due to rectangular shape of detectors and effects of magnetic field.

Due to less acceptance effects X component is used for $v_1$ and Y for $v_2$

# Sources of systematics: symmetry plane estimation

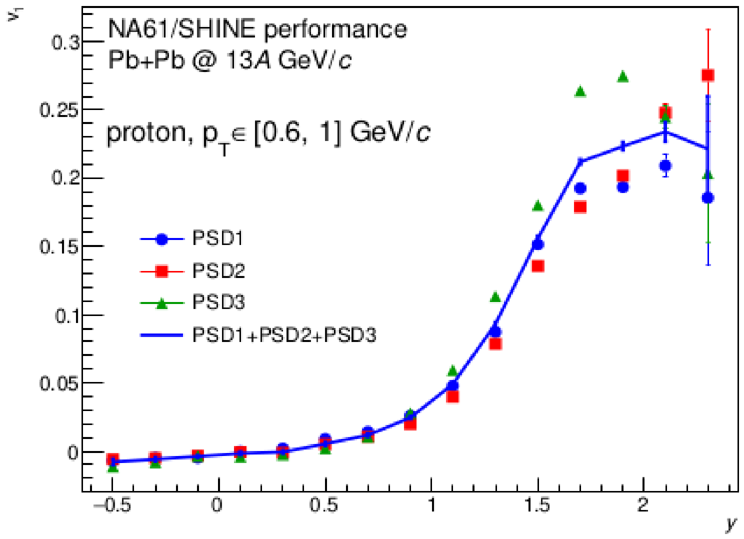


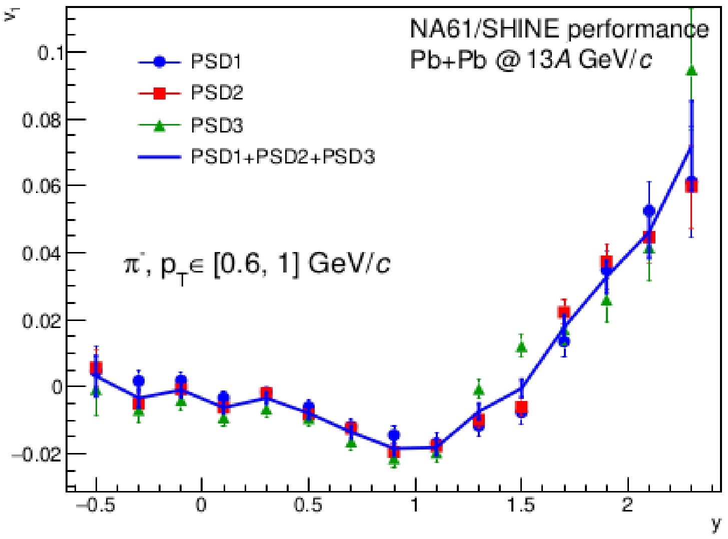


PSD

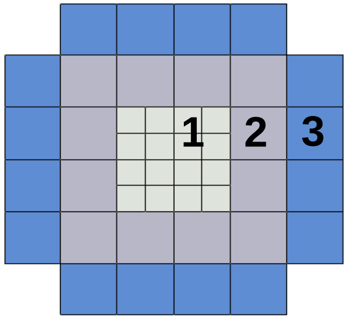


(non-flow correlations due to overlap between TPC and peripheral PSD modules)

# Results

# Proton directed flow

**13*A* GeV/*c***

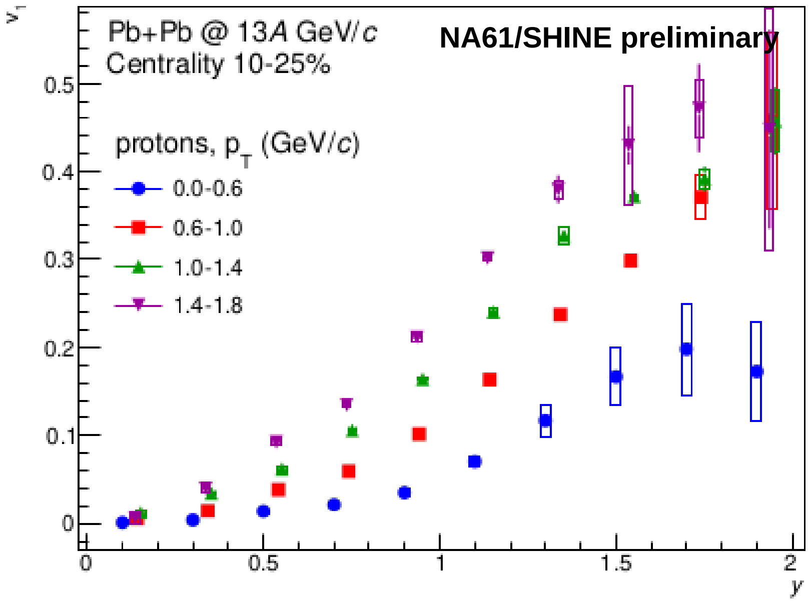


**30*A* GeV/*c***

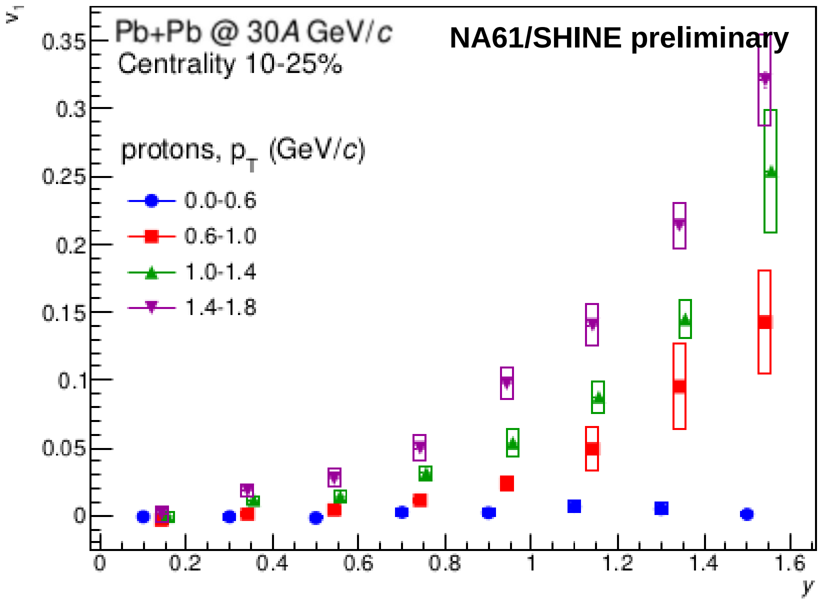


- Clear energy dependence due to change in spectator passing time

# Charged pion directed flow (low $p_T$)

**13*A* GeV/*c***

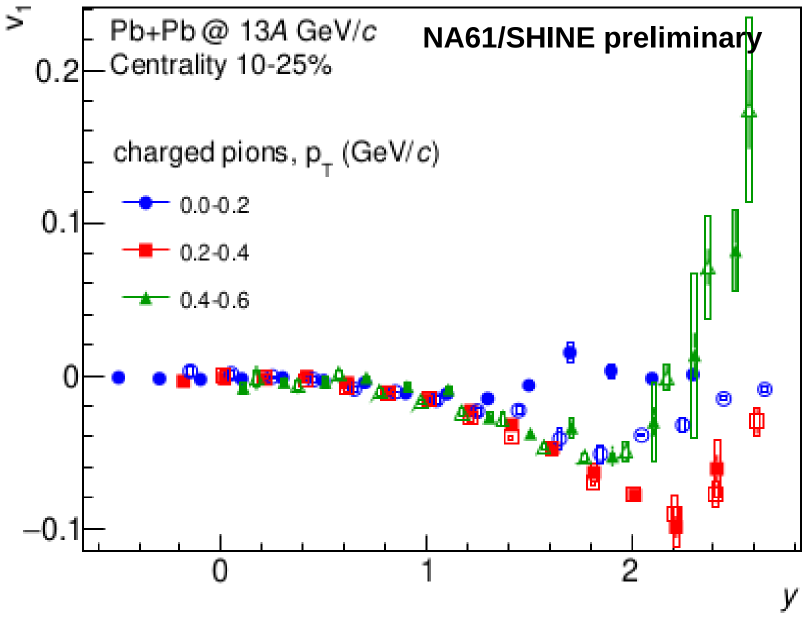


**30*A* GeV/*c***

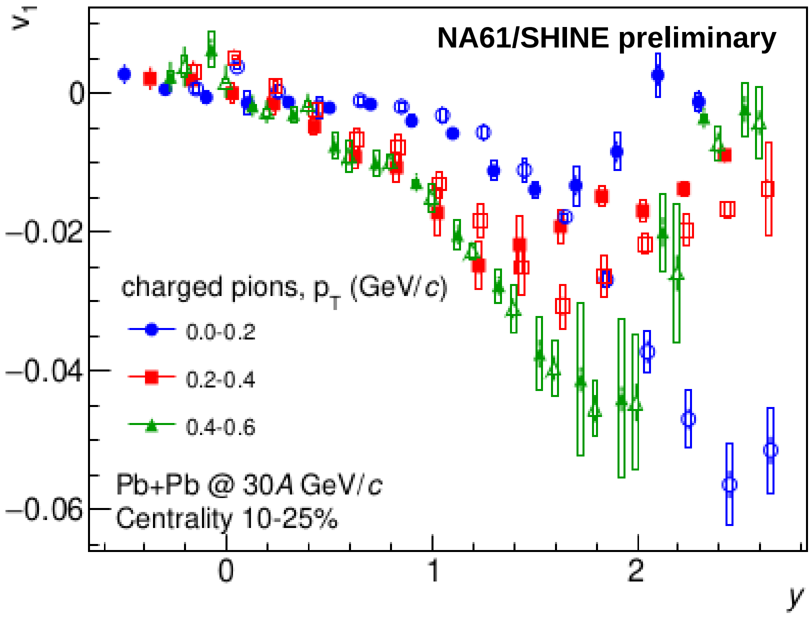


- Filled markers – $\pi^-$, open markers – $\pi^+$.

# Charged pion directed flow (low $p_T$)

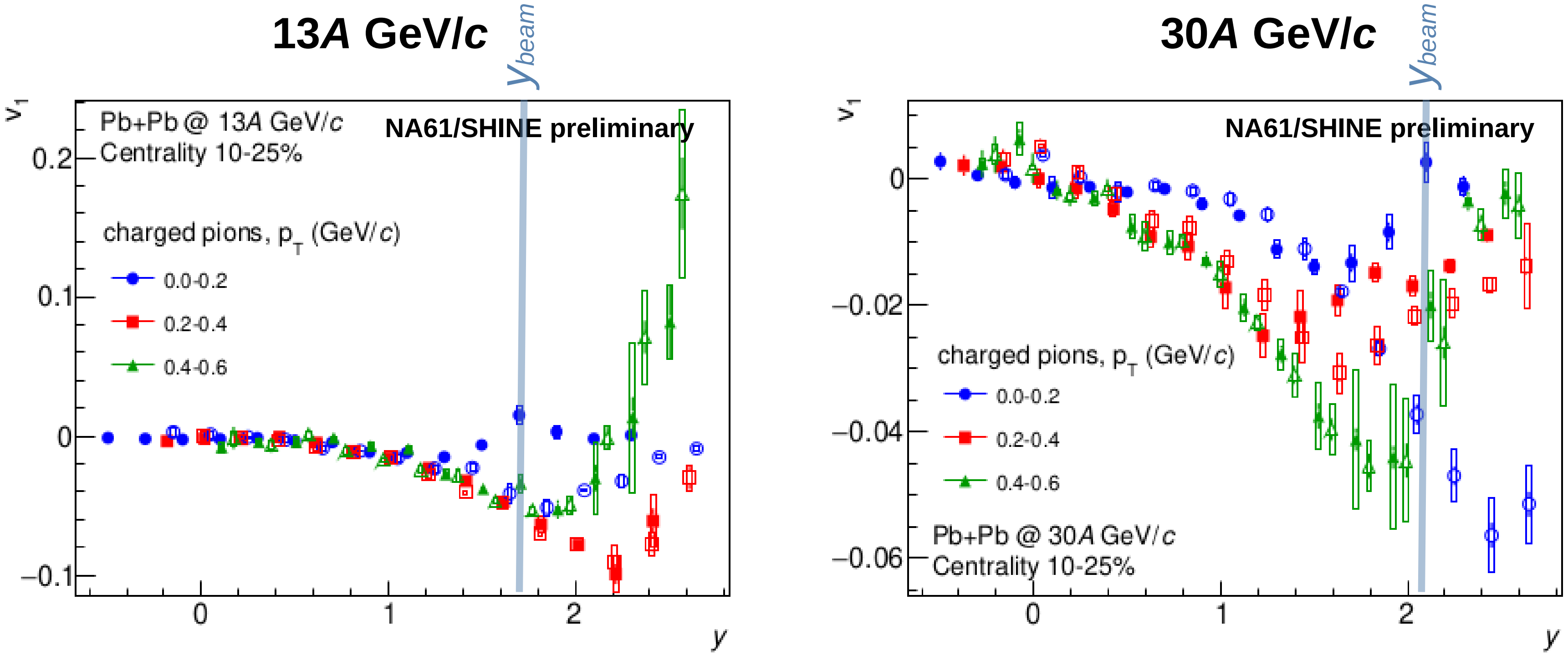


- Filled markers – $\pi^-$, open markers – $\pi^+$.
- Clear charge splitting close to beam rapidity at low $p_T$ - Coulomb interaction with spectators?

# Coulomb interaction with spectators: model calculations

**158*A* GeV/*c***

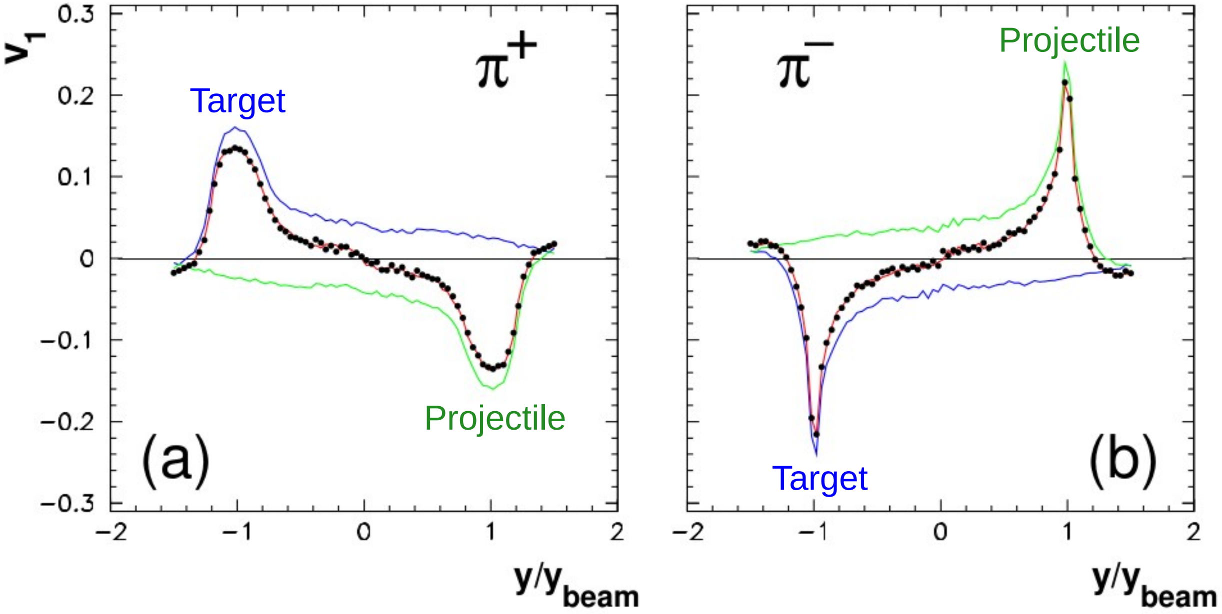


- Coulomb interaction with spectators produces pion $v_1$ in a model without flow
- Measurements may help to constrain pion emission time

A. Rybicki, A. Szczurek Phys. Rev. C 87, 054909 (2013)

# Charged pion directed flow (higher $p_T$)

**13*A* GeV/*c***

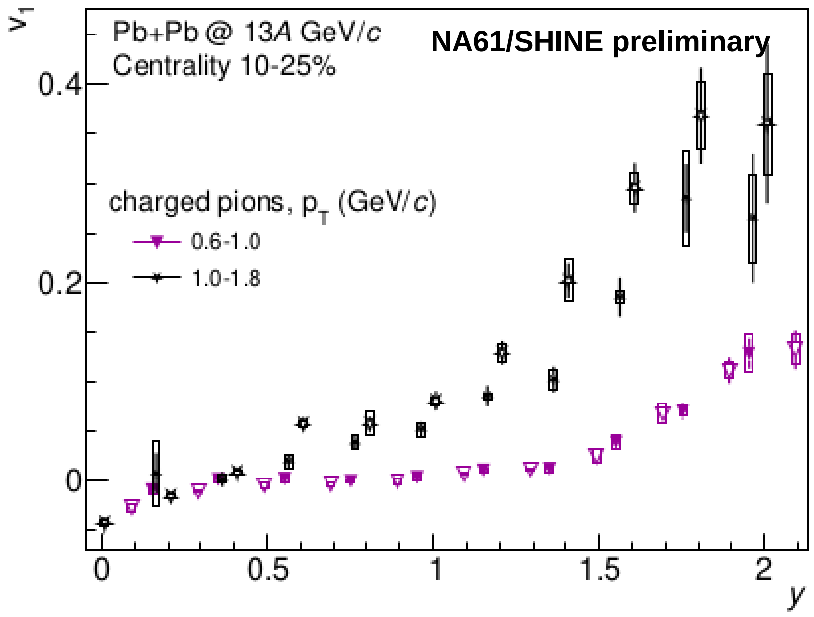


**30*A* GeV/*c***

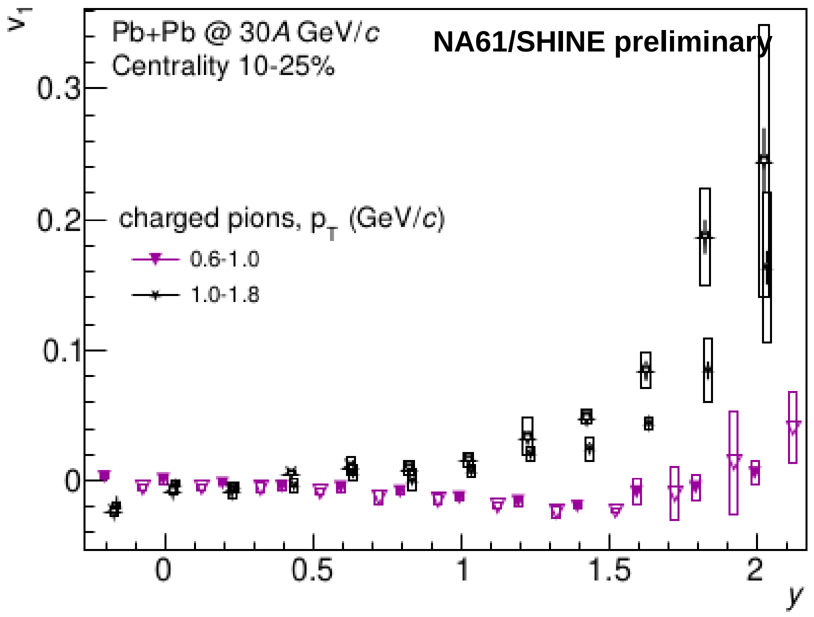


- Filled markers – $\pi^-$, open markers – $\pi^+$.
- Charge splitting disappears at higher $p_T$

# Slope of directed flow at midrapidity

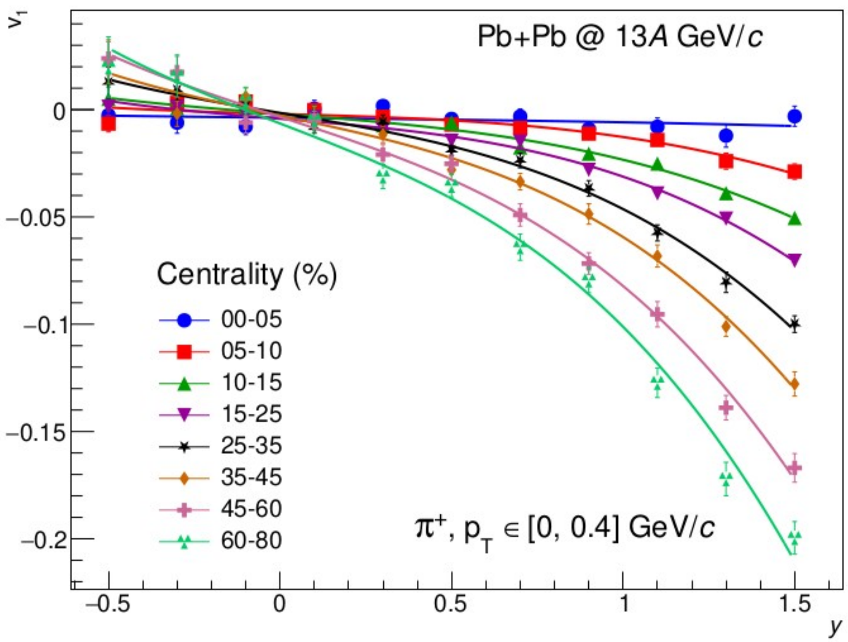


- Sensitive to the EoS
- Changes with centrality and $p_T$
- May vary with different fitting functions ($f=a+by+cy^3$ was used in this analysis)

# Slope of directed flow (13*A* GeV/*c*)

$p_T$ ϵ [0, 0.4] GeV/*c*

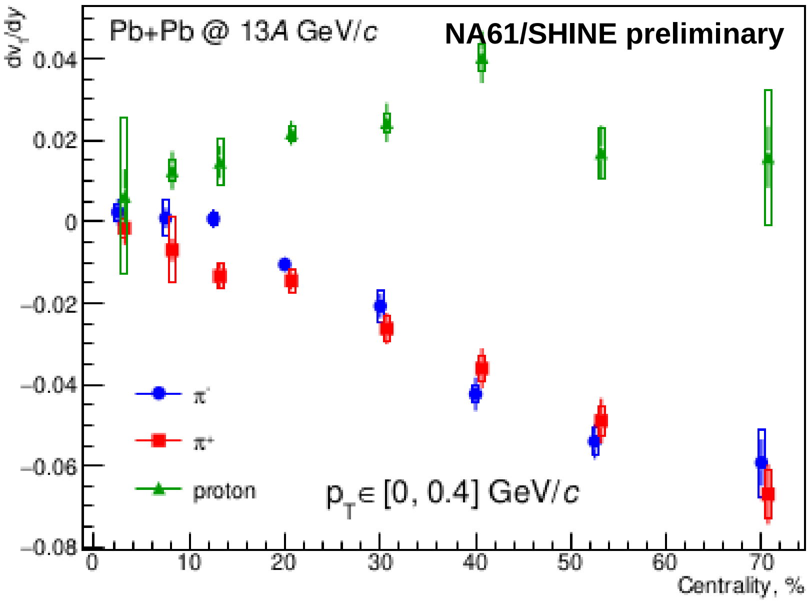


$p_T$ ϵ [0.4, 2] GeV/*c*

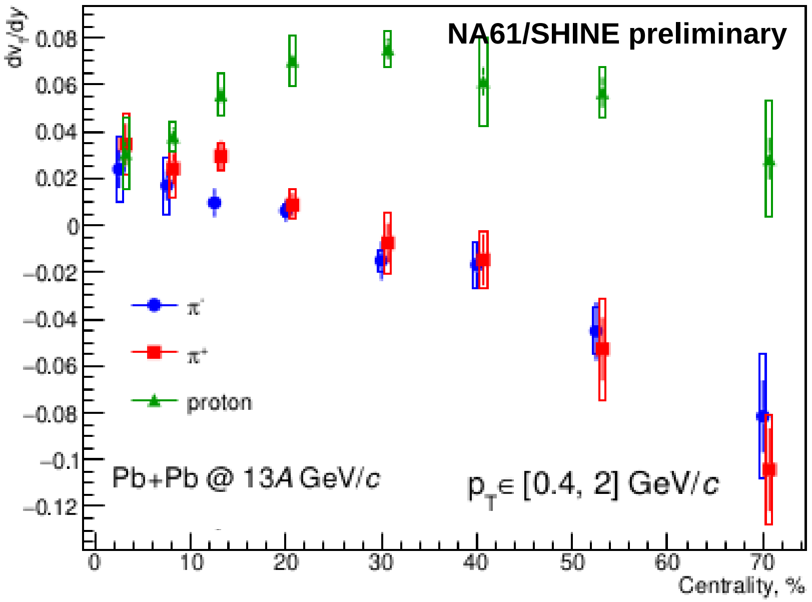


- Mostly positive sign for protons and negative for pions
- Weak centrality dependence of proton slope

# Slope of directed flow (30*A* GeV/*c*)

$p_T$ ϵ [0, 0.4] GeV/*c*

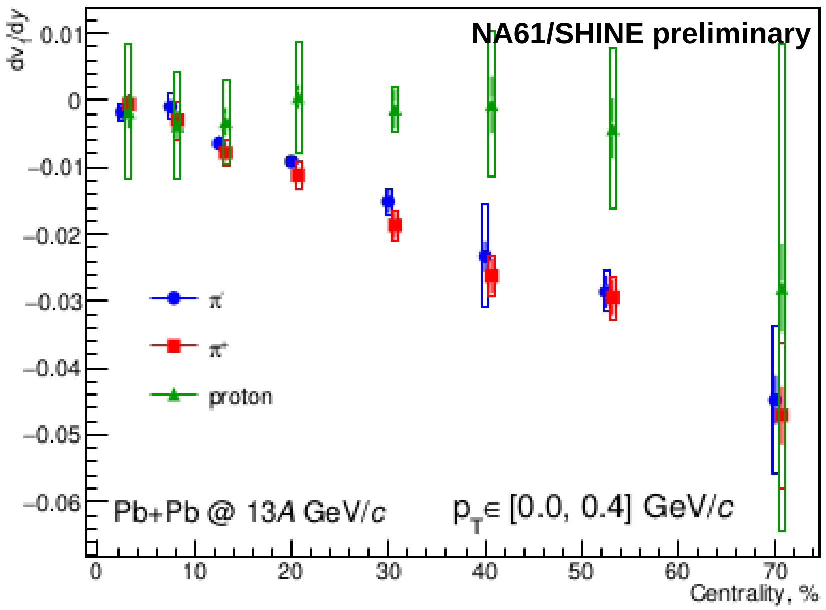


$p_T$ ϵ [0.4, 2] GeV/*c*

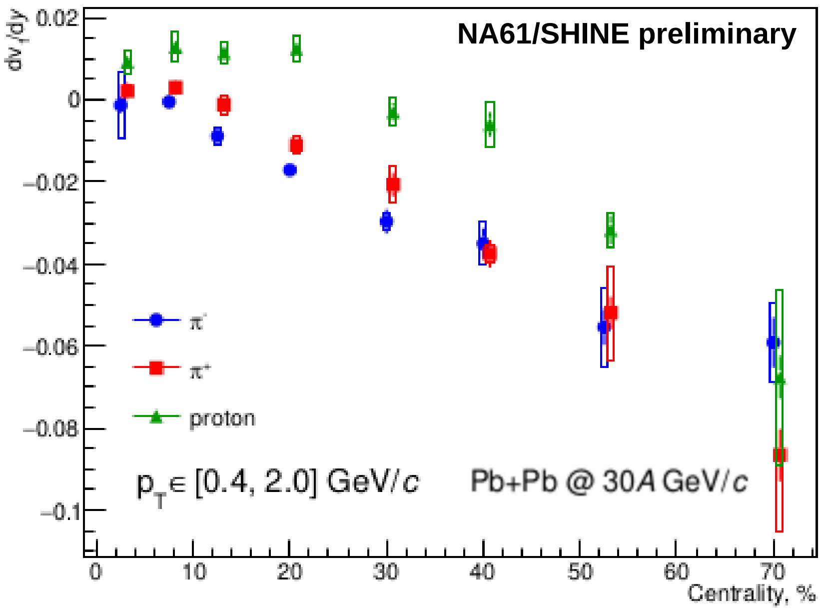


- Proton slope is comparable with zero for lower $p_T$
- At higher $p_T$ proton slope changes sign around 40% centrality – could be a hint of EoS softening or reflect the increase in angular momentum

# Slope of directed flow: world data

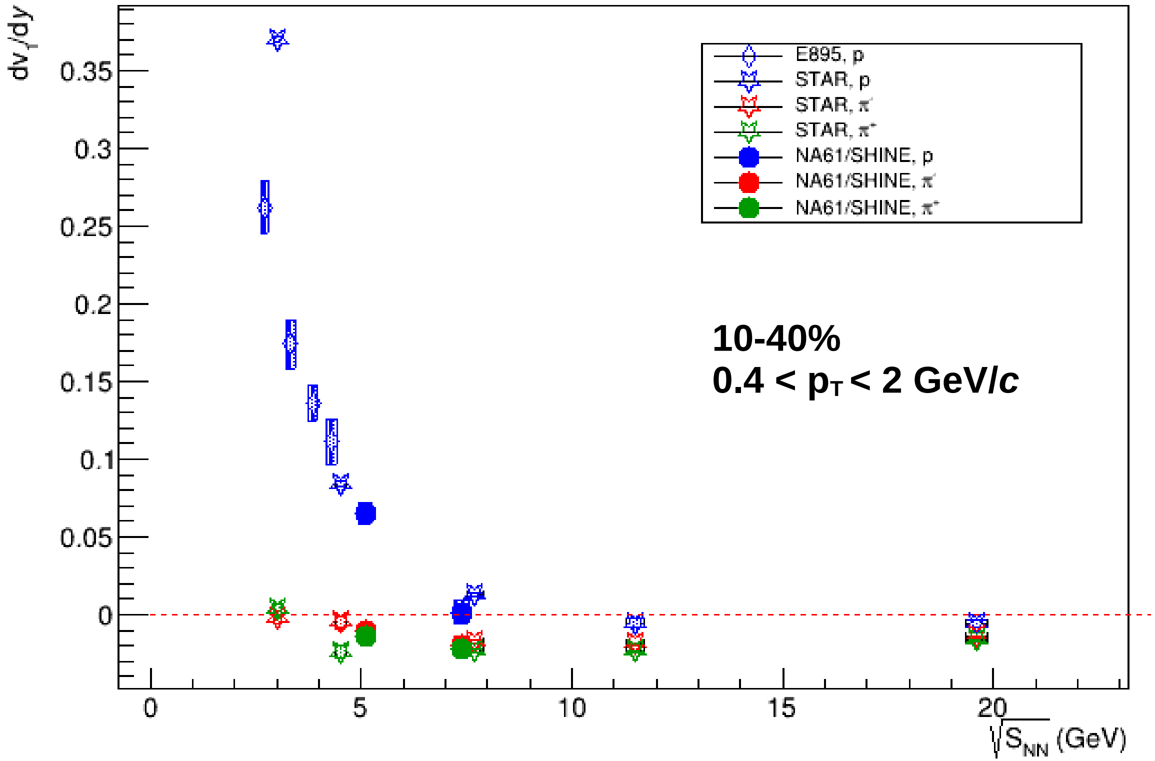


- Results are in good agreement with STAR+E895 data
- **NB:** STAR points at 4.5 GeV are measured at 0-30% centrality

# Proton and charged pion elliptic flow

**13*A* GeV/*c***

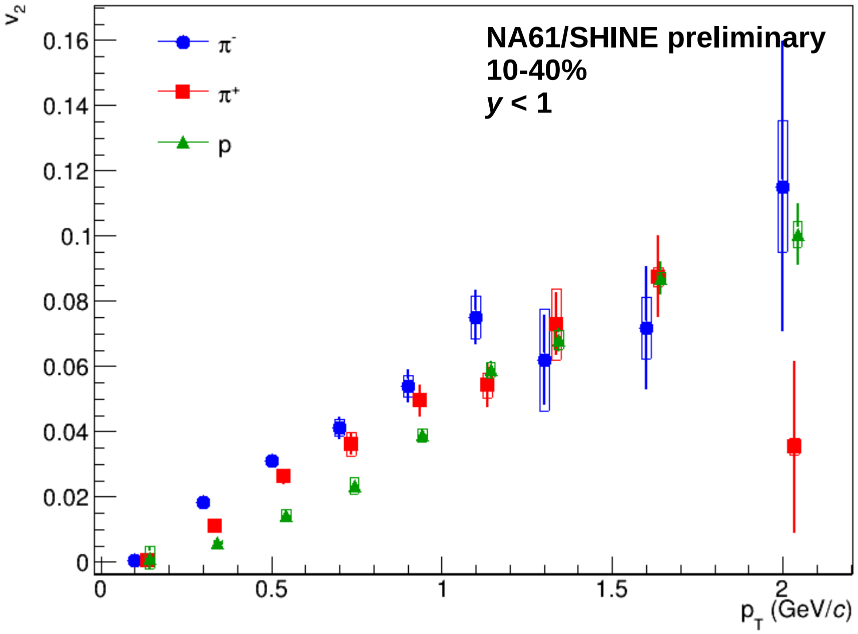


**30*A* GeV/*c***

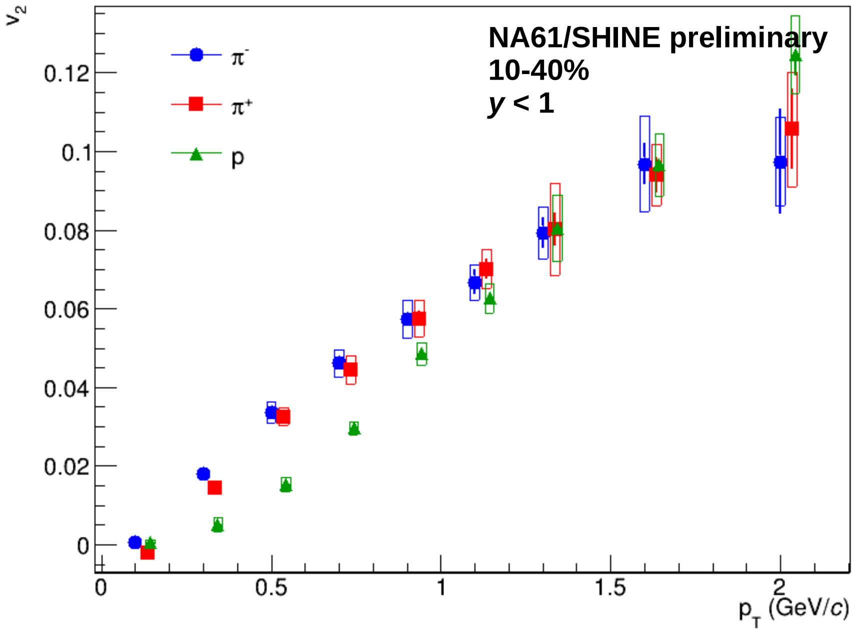


- Visible energy dependence of charged pion and proton elliptic flow

# Proton elliptic flow vs STAR results

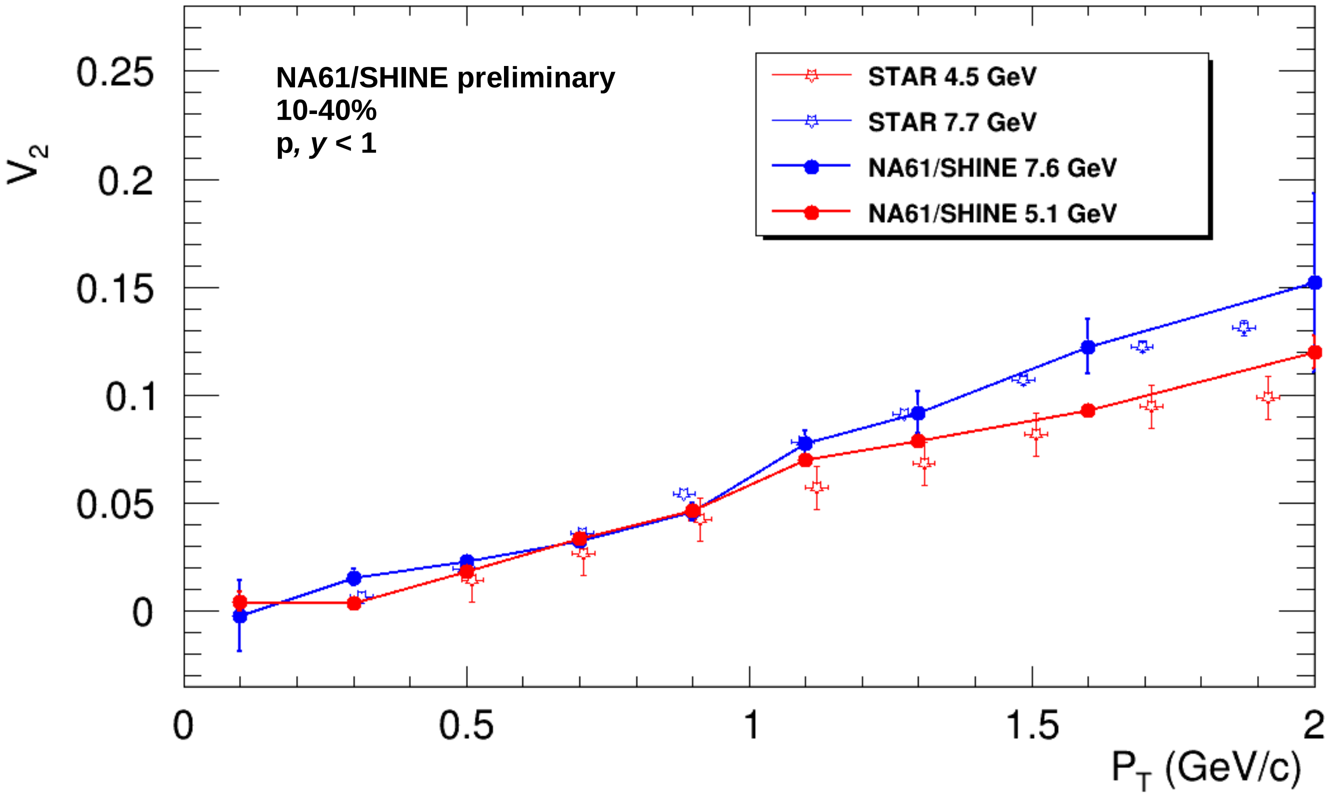


- Good agreement for both energy points

# Model comparison: DCM-QGSM-SMM

**p**

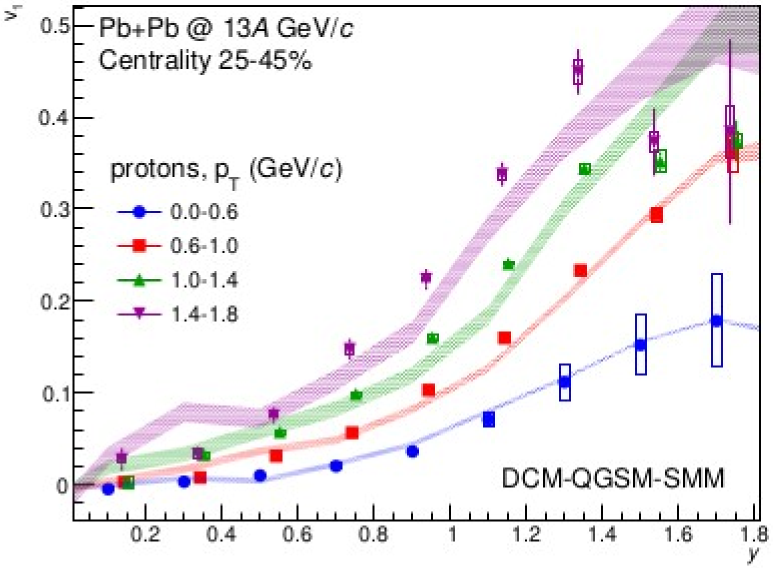


**π⁻**

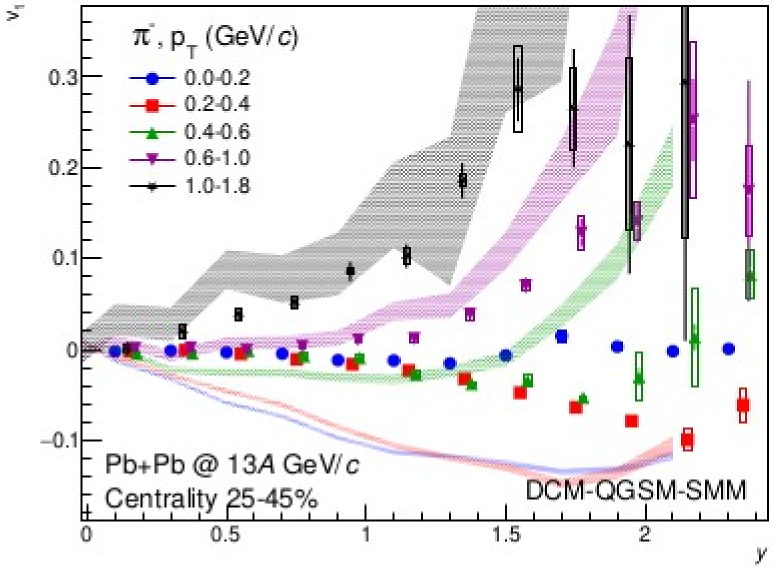


- Good agreement for proton $v_1$
- Pion $v_1$ is not well described at low $p_T$ with cascade models

# Model comparison: JAM

**p**

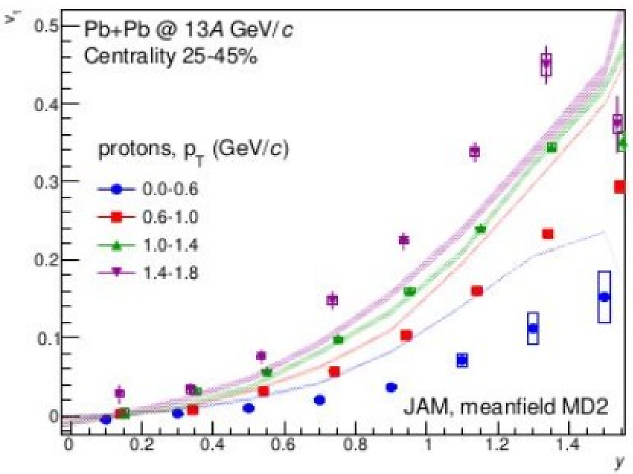


**$\pi^-$**

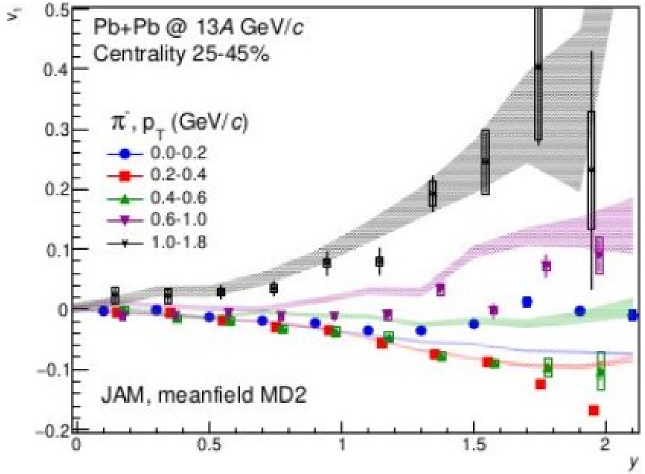


**$\pi^+$**

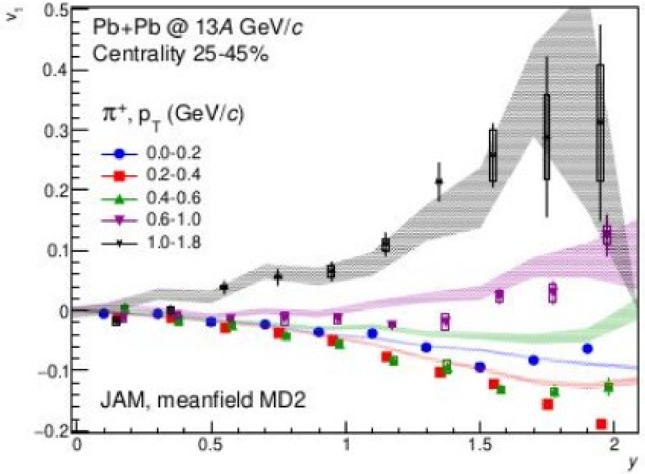


- Meanfield regime, MD2 EoS
- Limited agreement for proton $v_1$ differential results
- Pion $v_1$ is well reproduced except for charge splitting

# Summary

- Highly differential $v_1$ measurements performed for protons and charged pions in Pb+Pb collisions at 13A and 30A GeV/*c*
- Two energy points added to $v_1$ slope of protons and charged pions, in agreement with the world data.
- Charge splitting is shown for pion $v_1$ at lower $p_T$ close to beam rapidity, the results could help to constrain pion emmission time.
- Comparison with models shows the lack of agreement with highly differential measurements and neglect of Coulomb effect on charged pion $v_1$.
- $v_2$ measurements in wide kinematic bins show clear energy dependence and agree with the world data